Histamine H1 Receptors in Neural Stem Cells Are Required for the Promotion of Neurogenesis Conferred by H3 Receptor Antagonism following Traumatic Brain Injury

Rujia Liao,[1] Youchao Chen,[1] Li Cheng,[1] Lishi Fan,[1] Han Chen,[1] Yushan Wan,[1] Yi You,[1] Yanrong Zheng,[1] Lei Jiang,[1] Zhong Chen,[1] Xiangnan Zhang,[1,*] and Weiwei Hu[1,2,*]

[1]Department of Pharmacology, NHC and CAMS Key Laboratory of Medical Neurobiology, School of Basic Medical Science, College of Pharmaceutical Sciences, Zhejiang University, Hangzhou, Zhejiang 310058, P.R. China
[2]Pharmacy of Second Affiliated Hospital, Zhejiang University, Hangzhou, Zhejiang 310009, P.R. China
*Correspondence: xiangnan_zhang@zju.edu.cn (X.Z.), huww@zju.edu.cn (W.H.)
https://doi.org/10.1016/j.stemcr.2019.01.004

SUMMARY

The neurological recovery following traumatic brain injury (TBI) is limited, largely due to a deficiency in neurogenesis. The present study explores the effects of histamine H3 receptor (H3R) antagonism on TBI and mechanisms related to neurogenesis. H3R antagonism or *H3R* gene knockout alleviated neurological injury in the late phase of TBI, and also promoted neuroblast differentiation to enhance neurogenesis through activation of the histaminergic system. Histamine H1 receptor, but not H2 receptor, in neural stem cells is shown to be essential for this promotion by using *Hrh1$^{fl/fl}$;Nestin^{CreERT2}* and *Hrh2$^{fl/fl}$;Nestin^{CreERT2}* mice. Moreover, increase in mature and functional neurons at the penumbra area conferred by H3R antagonism was abrogated in *Hrh1$^{fl/fl}$;Nestin^{CreERT2}* mice. Taken together, H3R antagonism provides neuroprotection against TBI in the late phase through the promotion of neurogenesis, and the H1 receptor in neural stem cells is required for this action. H3R may serve as a new target for clinical treatment of TBI.

INTRODUCTION

Current medical management of acute traumatic brain injury (TBI) is primarily supportive, aimed at reducing intracranial pressure and optimizing cerebral perfusion (Levin and Diaz-Arrastia, 2015). There are no pharmacological therapies to date that have been unequivocally demonstrated to improve neurological outcomes in the late phase of TBI (Blennow et al., 2012; Xiong et al., 2010). Neurogenesis contributes to the functional repair of the central nervous system (CNS) through the processes of generation, migration, differentiation, and functional integration of newborn neurons into the pre-existing neuronal network (Zhao et al., 2008). Neurogenesis-related therapies involve (1) the administration of pro-neurogenic factors to boost endogenous mobilization of these neuronal precursors, (2) the transplantation of exogenous stem cells, and (3) a newly developed approach to reprogramming (Blaya et al., 2015; Hallbergson et al., 2003). However, transplantation has several limitations, such as short half-lives, limited diffusion of transplanted cells in CNS parenchyma, prolonged host immune responses, and tumorigenicity (Trounson and McDonald, 2015). The reprogramming approach often requires genetic manipulation, which is not easily accomplished in humans (Li and Chen, 2016). Present pro-neurogenic factors are less aggressive, but most are proteins also having the disadvantage of short half-life and limited penetration of the blood-brain barrier. There is thus a potential value in better therapeutic interventions aimed at supporting the endogenous neurogenic response for neurological recovery from TBI. In particular, specific targets are needed to prevent adverse effects on existing neurons or other cells (Li and Chen, 2016).

Accumulating evidence suggests that the histaminergic system may have a role in the regulation of brain injury (Hu and Chen, 2017; Liao et al., 2015). Histamine can increase proliferation and differentiation of neural stem cells (NSCs) derived from fetal rat cortex *in vitro* (Molina-Hernandez and Velasco, 2008; Rodriguez-Martinez et al., 2012). It has been reported that the action of histamine on neurogenesis is related to its postsynaptic histamine H1 receptor (H1R) or histamine H2 receptor (H2R) (Molina-Hernandez and Velasco, 2008). However, due to the unavailability of conditional knockout mice for H1R or H2R, the role of cell-type-specific histamine receptors in neurogenesis is still unclear. Moreover, the direct application of histamine is clinically limited due to its poor penetration of the blood-brain barrier and its pro-inflammatory effect. By virtue of the extensive CNS localization of the presynaptic autoreceptor histamine H3 receptor (H3R), its antagonists produce an almost unique activation of the histaminergic system in the brain (Haas and Panula, 2003).

H3R antagonism can prevent seizure development and improve working memory through the activation of histaminergic neurons (Huang et al., 2004; Zhang et al., 2003). In addition, we have recently found that H3R antagonism protects against ischemia-reperfusion injury via histamine-independent mechanisms (Yan et al., 2014). Despite the above-mentioned findings supporting H3R blockade as

generally neuroprotective via histamine-dependent or independent pathways, targeting of the H3R has not been viewed as a strategy for the treatment of TBI. It is thus imperative to explore the action of H3R antagonism and the role of the cell-type-specific postsynaptic histamine receptors in neurogenesis following TBI by selective deletion of H1R or H2R in NSCs or surrounding cells.

RESULTS

H3R Antagonism Provides Neuroprotection against TBI at the Late Phase

Two experimental TBI models were employed to investigate the effect of H3R antagonism on TBI. In the cryogenic lesion model, neurological function was robustly impaired at 1 day after TBI, with an increased time for traversal in the beam walk test (p < 0.001) and a decreased latency to fall off the wire lid in the wire hanging test (p < 0.001, Figure 1). Neurological function gradually recovered thereafter. A prominent lesion was found in the cortex as well, after TBI (Figure 1A). The H3R antagonist thioperamide significantly reduced the lesion volume and alleviated the neurological dysfunction at 28 days after TBI, but not in the early phase of TBI (Figures 1A–1C, S1A, and S1B; the lesion volume at 7 days after TBI was 17.56 ± 5.22 mm^3 for the thioperamide-treated group compared with 19.88 ± 4.74 mm^3 for the control group, p > 0.05). Thioperamide acted in a dose-dependent manner that can be reversed by the selective H3R agonist immepip (Figures 1A–1C, p < 0.05). Moreover, the deletion of the H3R gene (Hrh3) showed protection with respect to the lesion volume and neurological dysfunction in the late phase following TBI, although further augmentation of this protection was not observed after H3 antagonism by thioperamide in the $Hrh3^{-/-}$ mice (Figures 1D–1F, S1C, and S1D). Controlled cortical impact (CCI) injury was also employed, which displays cerebral injury more closely resembling those that are observed clinically (Smith et al., 1995; Xiong et al., 2013). Thioperamide also conferred similar protection from increased lesion volume and functional impairment in behavioral tests at 28 days after TBI (Figures 1G–1I). These data suggest that H3R antagonism provides neuroprotection against TBI in the late phase.

The Activation of the Histaminergic System and H1R in NSCs Is Required for the Promotion of Neurogenesis Conferred by H3R Antagonism after TBI

To determine whether the observed neuroprotection from H3R blockade is related to its promotion of neurogenesis, the numbers of neuroblasts in subventricular zones (SVZ) and subgranular zones (SGZ) were quantified by doublecor-tin (DCX) immunostaining. Wild-type (WT) mice that experienced cryogenic TBI showed no signs of increased neurogenesis compared with the sham group, whereas H3R antagonism by thioperamide increased the number of neuroblasts in SVZ and SGZ in a dose-dependent manner (Figures 2A and 2B). This action was inhibited by a co-treatment with immepip. When the H3R gene was deleted, the number of neuroblasts markedly increased, although thioperamide failed to further increase the number of neuroblasts in $Hrh3^{-/-}$ mice (Figures 2A and 2B). This result suggests that H3R blockade promoted neurogenesis after TBI.

To explore whether histamine and its receptors are involved in this effect, the HDC inhibitor α-fluoromethyl-histidine (α-FMH) and a knockout mutation of the HDC gene were employed to block the synthesis of histamine. The increase in neuroblasts induced by thioperamide was no longer observed following deletion of HDC or treatment with α-FMH (Figures 2A and 2C). Furthermore, the H1 antagonist pyrilamine, but not the H2 antagonist cimetidine, can reverse the action of thioperamide (Figures 2A and 2C). Also, pyrilamine but not cimetidine prevented the reduction of lesion volume and the amelioration of neurological function conferred by thioperamide (Figures 2D–2F). In addition, no alteration was observed in the number of neuroblasts in mice with TBI after treatment with immepip, α-FMH, pyrilamine, or cimetidine (data not shown). This suggests that activation of the histaminergic system and then H1R is involved in the neuroprotection provided by H3R antagonism.

H1R and H2R are located not only in NSCs and derived newborn cells, but also in surrounding CaMKIIα$^+$ glutamatergic neurons. To identify whether H1R in NSCs is critical for the neurogenesis and protection conferred by H3R blockade, $Hrh1^{fl/fl};Nestin^{CreERT2}$, $Hrh2^{fl/fl};Nestin^{CreERT2}$, and $Hrh1^{fl/fl};CaMKIIα^{Cre}$ mice were used here. Interestingly, thioperamide failed to promote neurogenesis in $Hrh1^{fl/fl};Nestin^{CreERT2}$ mice but not in $Hrh2^{fl/fl};Nestin^{CreERT2}$ mice after tamoxifen induction (Figures 3A and 3B). Meanwhile, from in situ hybridization of Hrh1 or Hrh2 mRNA expression, the deletion of H1R and H2R was found in these neuroblasts (Figure S2A). Furthermore, the reduction of lesion volume and the amelioration of neurological function conferred by thioperamide were no longer obtained in $Hrh1^{fl/fl};Nestin^{CreERT2}$ mice but were preserved in their $Nestin^{CreERT2}$ littermates (Figures 3D–3F).

In addition, thioperamide showed comparable promotion of neurogenesis in $Hrh1^{fl/fl};CaMKIIα^{Cre}$ mice, suggesting that H1R in surrounding CaMKIIα$^+$ glutamatergic neurons is not involved in the amplification of neurogenesis provided by thioperamide (Figures S2B–S2D). The above data suggest that H1R in NSCs is required for the neuroprotection and promotion of neurogenesis conferred by H3R antagonism after TBI.
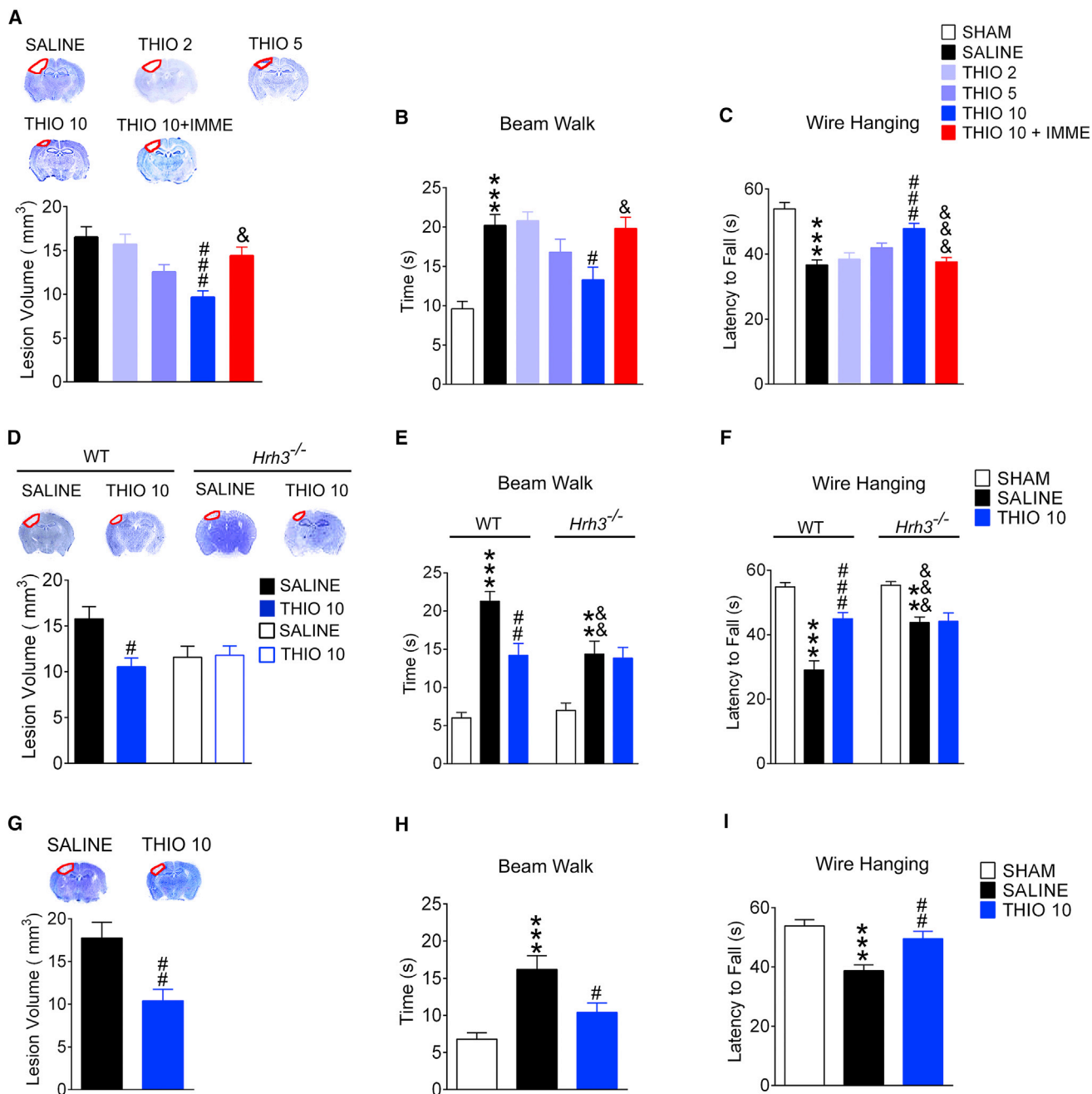
Figure 1. Histamine H3R Antagonism Provides Neuroprotection against TBI in the Late Phase

Wild-type (WT) (A–I) or *Hrh3*$^{-/-}$ mice (D–F) were exposed to cryogenic brain lesions (A–F) or controlled cortical impact injuries (G–I), and then treated with saline, or H3R antagonist thioperamide (THIO; 2, 5, or 10 mg/kg/day, intraperitoneally), or THIO together with H3R agonist immepip (IMME; 1 mg/day, intracerebroventricularly). The neurological function in beam walk (B, E, and H) or wire hanging tests (C, F, and I) at 28 days after TBI is shown, while the lesion volumes are shown in (A), (D), and (G). (A–C) n = 10–11; (D–I) n = 9–11. Data are represented as means ± SEM. **p < 0.01, ***p < 0.001 versus the sham group; #p < 0.05, ##p < 0.01, ###p < 0.001 versus the SALINE group; &p < 0.05, &&p < 0.01, &&&p < 0.001 versus the THIO 10 group in (A)–(C) or the SALINE group in WT mice in (E) and (F). See also Figure S1.
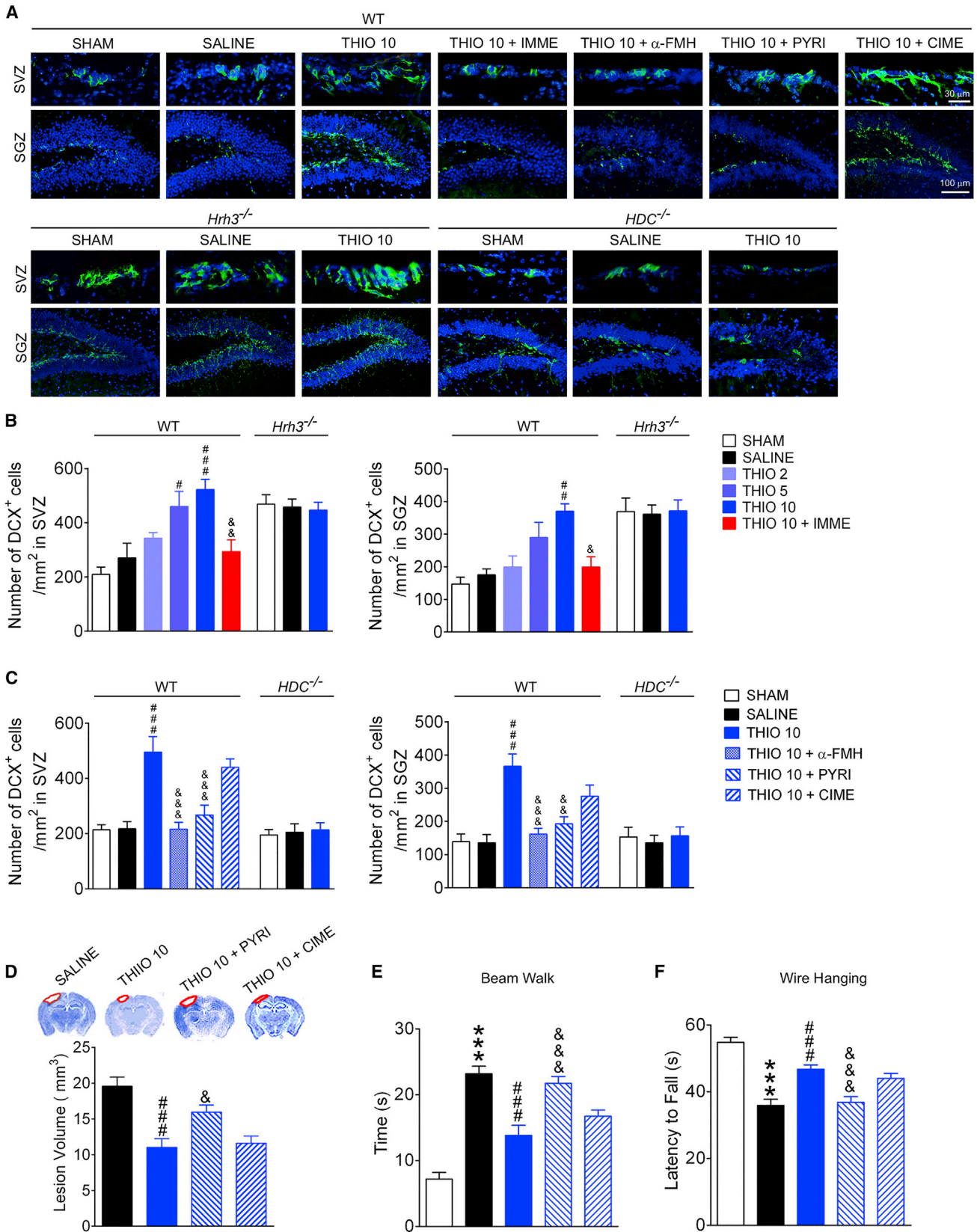
(legend on next page)

The H1R Is Required for the Promotion of Neural Stem Cell Differentiation Conferred by H3R Antagonism after TBI

In the adult SVZ and SGZ, self-renewing NSCs give rise to neuroblasts; therefore the increased number of neuroblasts could result either from increased proliferation or from promoted differentiation. We found that there is no difference in the number of Nestin$^+$ NSCs between saline- and thioperamide-treated WT mice following TBI (Figures S3A and S3B). The mice treated with thioperamide also have similar levels of bromodeoxyuridine$^+$ (BrdU) proliferating cells and PCNA$^+$/DCX$^+$ proliferating neuroblasts in SVZ and SGZ (Figures S3C–S3F). These data indicate that H3R antagonism has no effect on the proliferation of NSCs, including those that have developed into neuroblasts. Furthermore, TUNEL analysis was performed to exclude the increase in neuroblasts after H3R antagonism caused by a reduction of apoptosis. We found that TUNEL$^+$ cells were observed in the lesion area, but were seldom found in the SVZ and SGZ (Figure S3G), suggesting that the promotion of neurogenesis conferred by H3R antagonism is not related to a protection of neuroblasts against apoptosis.

To identify whether H3R antagonism promotes neural differentiation, the cell morphology features of neuroblasts, such as dendritic growth, were analyzed after immunostaining with DCX and polysialylated neuronal cell adhesion molecule (PSA-NCAM) (Figure 4). In the TBI group, the neuroblasts showed a characteristic stellate morphology with several short processes (Figure 4A). However, the leading process length (the future apical dendrite) and the total branch length of neuroblasts were robustly increased in thioperamide-treated mice (Figures 4A and 4B). Importantly, the effect of thioperamide on neural differentiation was lost in $Hrh1^{fl/fl};Nestin^{CreERT2}$ mice, but not in $Hrh2^{fl/fl};Nestin^{CreERT2}$ mice, regarding the length of leading processes and total branch length (Figures 4C and 4D). These findings suggest that the H1R in NSCs is required for the promotion of its differentiation provided by H3R antagonism. Since NSCs also express H3R (Escobedo-Avila et al., 2014; Molina-Hernandez and Velasco, 2008), we examined a direct effect of H3R- or H1R-related drugs and knockdown of H3R on NSC differentiation *in vitro* to further confirm that H1R, but not H3R, in NSCs is involved

in the promotion of neurogenesis conferred by H3 antagonists. We found that both histamine and the H1 agonist histamine trifluoromethyl toluidide (HTMT), but not thioperamide, promoted NSC differentiation (Figures S4A, S4B, S4D, and S4E). Moreover, the H1 antagonist pyrilamine, but not H2 or H3 antagonists, abrogated the promotion of the NSC differentiation provided by histamine (Figures S4A and S4C). The NSCs from $Hrh3^{fl/fl}$ mice were transfected with $AAV-CAG-EGFP-Cre$ to knock down H3R expression, which was confirmed by *in situ* hybridization of $Hrh3$ mRNA (Figures S4F and S4G). There was no difference in NSC differentiation between EGFP$^+$ NSCs that had knockdown of H3R and EGFP$^-$ control NSCs (Figures S4H and S4I), suggesting that the H3R in NSCs may not be involved in their differentiation. The above results support the critical role of H1R in NSCs in the promotion of neurogenesis conferred by H3 antagonists.

The H1R in Newly Generated Cells Is Critical for Differentiation into Functional Neural Cells Conferred by H3R Antagonism

Although an increase in the number of neuroblasts was detected after H3R antagonism, whether these immature cells migrate and differentiate into mature neurons at the penumbra area to integrate into the neural network is still unknown. A pROV-EF1a-GFP retrovirus was used to trace newly generated cells by direct injection of the virus into the SVZ or SGZ 5 days before TBI (Figure S5). More newly generated GFP$^+$ cells were then found at the penumbra area after thioperamide treatment, which were recruited from either the SVZ or the SGZ (Figures 5A and 5B). The fate of those newly generated cells at the penumbra area was determined by immunostaining with NeuN, S100β, or CC1 to label mature neurons, astrocytes, and oligodendrocytes, respectively. Although thioperamide significantly increased the number of newly generated cells in each type, it had no effect on their composition (Figures 5C, 5D, and 5F). Since CaMKIIα$^+$ glutamatergic neurons are the main type of excitatory neurons in the cortex, and parvalbumin (PV)$^+$ neurons are the main type of inhibitory neurons, we further analyzed the compositions of these two types of neurons and found that thioperamide did not change the percentages of CaMKIIα$^+$ glutamatergic

---

Figure 2. Histamine H3 Receptor Antagonism Promotes Neurogenesis in the SVZ and SGZ through the Activation of the Histaminergic System

WT (A–F), $Hrh3^{-/-}$ (A and B), or $HDC^{-/-}$ (A and C) mice were treated with saline, H3R antagonist thioperamide (THIO; 2, 5, or 10 mg/kg/day, intraperitoneally [i.p.]), or THIO together with H3R agonist immepip (IMME; 1 μg/day, intracerebroventricularly [i.c.v.]), α-FMH (5 μg/day, i.c.v.), pyrilamine (PYRI; 10 mg/kg/day, i.p.), or cimetidine (CIME; 10 mg/kg/day, i.p.) after cryogenic brain lesion. Fourteen days later, the number of DCX$^+$ neuroblasts in the SVZ and SGZ were counted (B and C), with representative photographs shown in (A). The neurological function in beam walk (E) or wire hanging tests (F) at 28 days after TBI is shown, while the lesion volumes are shown in (D). (A–C) n = 6–8; (D–F) n = 10–12. Data are represented as means ± SEM. ***p < 0.001 versus the sham group; #p < 0.05, ##p < 0.01, ###p < 0.001 versus the SALINE group; &p < 0.05, &&p < 0.01, &&&p < 0.001 versus the THIO 10 group in WT mice.
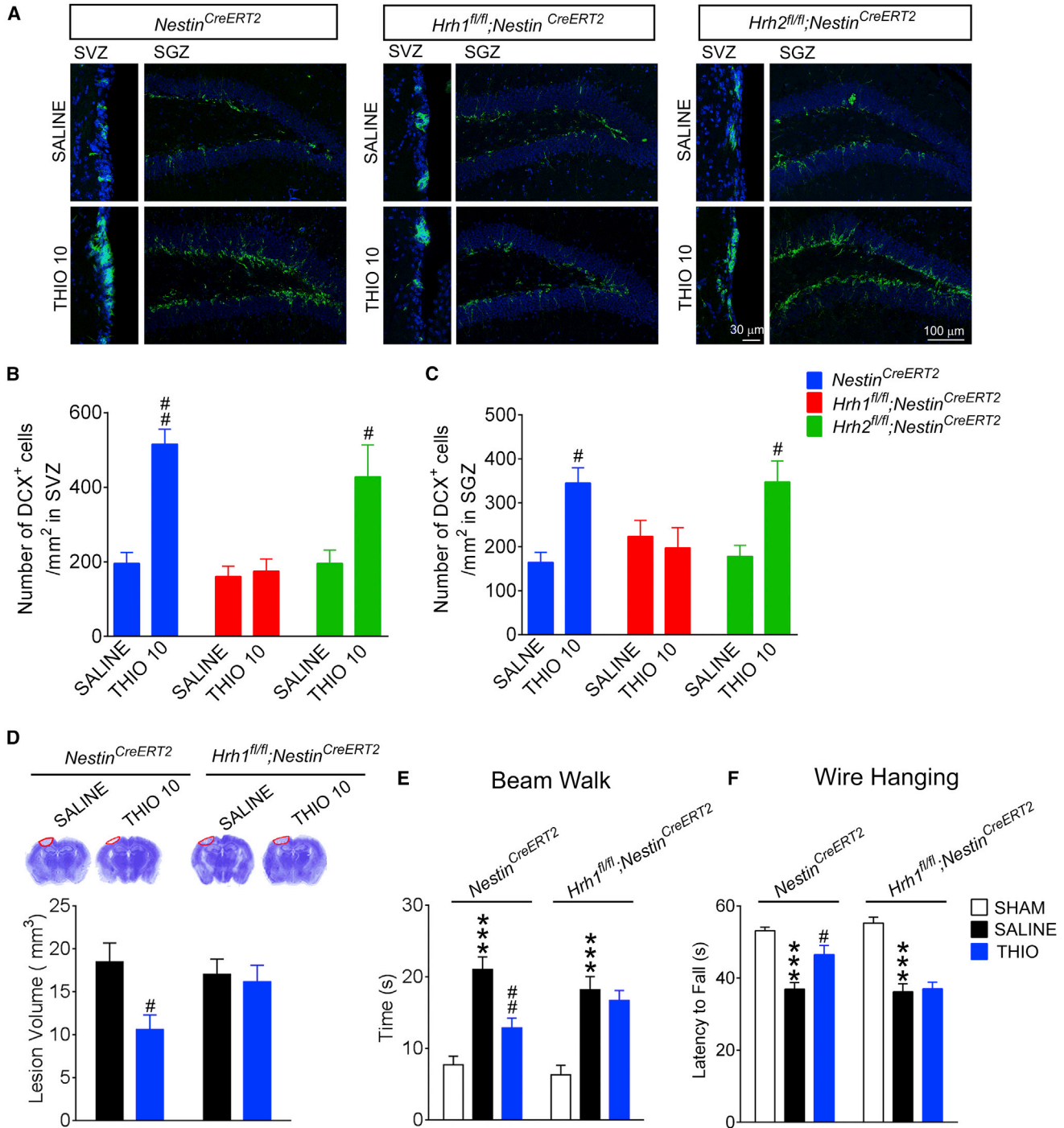
Figure 3. H1R but Not H2R in NSCs Is Required for the Neurogenesis and Neuroprotection Conferred by H3R Antagonism following TBI

$Hrh1^{fl/fl};Nestin^{CreERT2}$ and $Hrh2^{fl/fl};Nestin^{CreERT2}$ mice and their $Nestin^{CreERT2}$ littermates were treated with saline or thioperamide (10 mg/kg/day, i.p.) after cryogenic brain lesion. The numbers of DCX$^+$ neuroblasts in the SVZ (B) and SGZ (C) 14 days later are shown, with representative photographs in (A). The neurological function in beam walk (E) or wire hanging tests (F) at 28 days after TBI is shown, while the lesion volumes are shown in (D). (B and C) n = 5–6; (D–F) n = 8–12. Data are represented as means ± SEM. ***p < 0.001 versus the sham group of the same species; #p < 0.05, ##p < 0.01 versus the SALINE group of the same species. See also Figure S2.
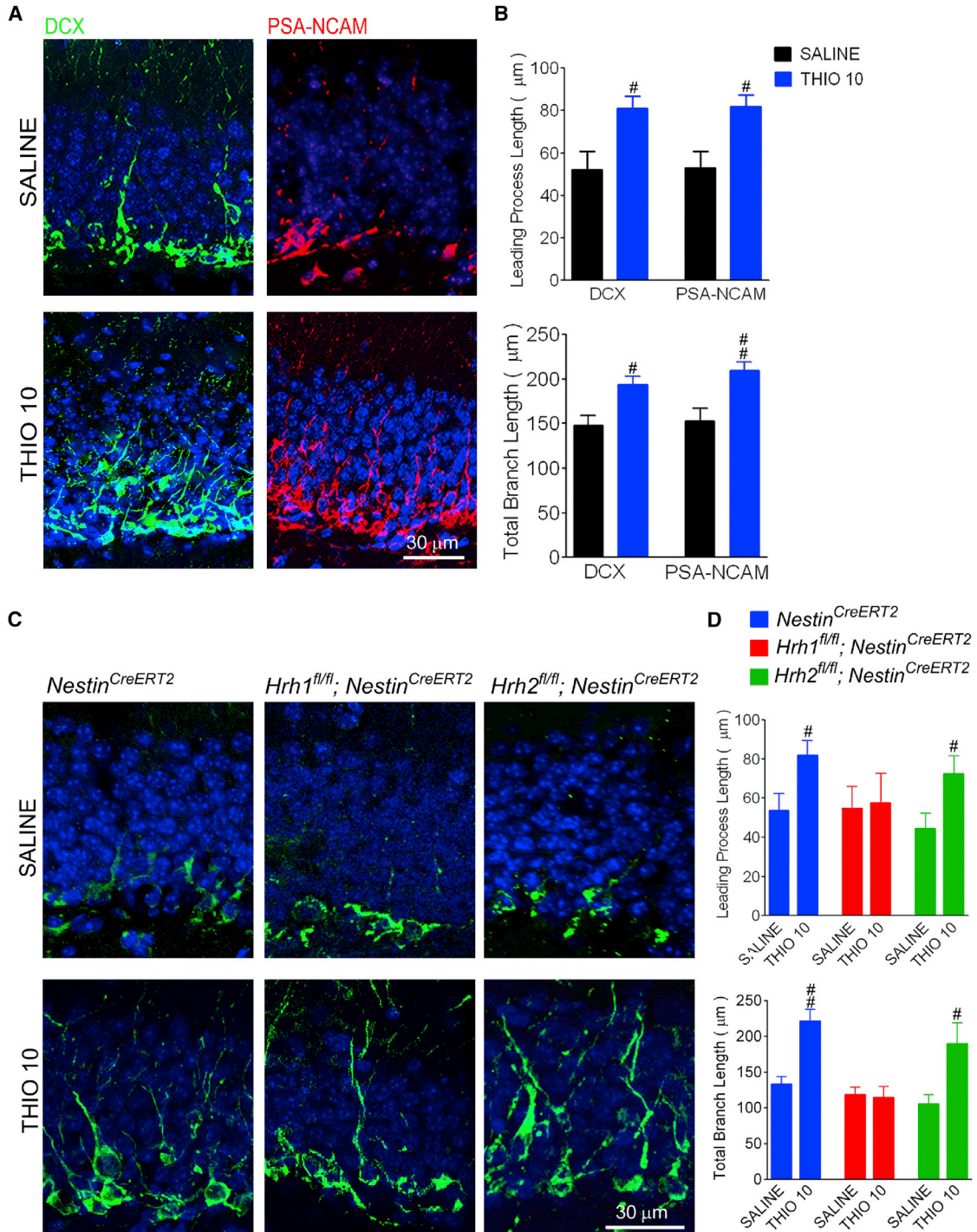
Figure 4. H3 Receptor Antagonism Promotes Neural Differentiation through H1R in NSCs following TBI

WT, $Hrh1^{fl/fl}$;$Nestin^{CreERT2}$, and $Hrh2^{fl/fl}$;$Nestin^{CreERT2}$ mice and their $Nestin^{CreERT2}$ littermates were treated with saline or H3R antagonist thioperamide (THIO; 10 mg/kg/day, i.p.) after cryogenic brain lesion. Confocal fluorescence microscopy images show longer process morphology of DCX+ or PSA-NCAM+ neuroblasts at 14 days after TBI in WT, $Nestin^{CreERT2}$, or $Hrh1^{fl/fl}$;$Nestin^{CreERT2}$ mice treated with thioperamide, but not in $Hrh2^{fl/fl}$;$Nestin^{CreERT2}$ mice (A and C). Image analysis of leading processes and total branch lengths shows greater lengths in THIO 10-treated neuroblasts in WT, $Nestin^{CreERT2}$, or $Hrh1^{fl/fl}$;$Nestin^{CreERT2}$ mice, but not in $Hrh2^{fl/fl}$;$Nestin^{CreERT2}$ mice using both DCX and PSA-NCAM staining (B and D). n = 5–6. #$p < 0.05$, ##$p < 0.01$ versus the SALINE group of the same species. See also Figures S3 and S4.
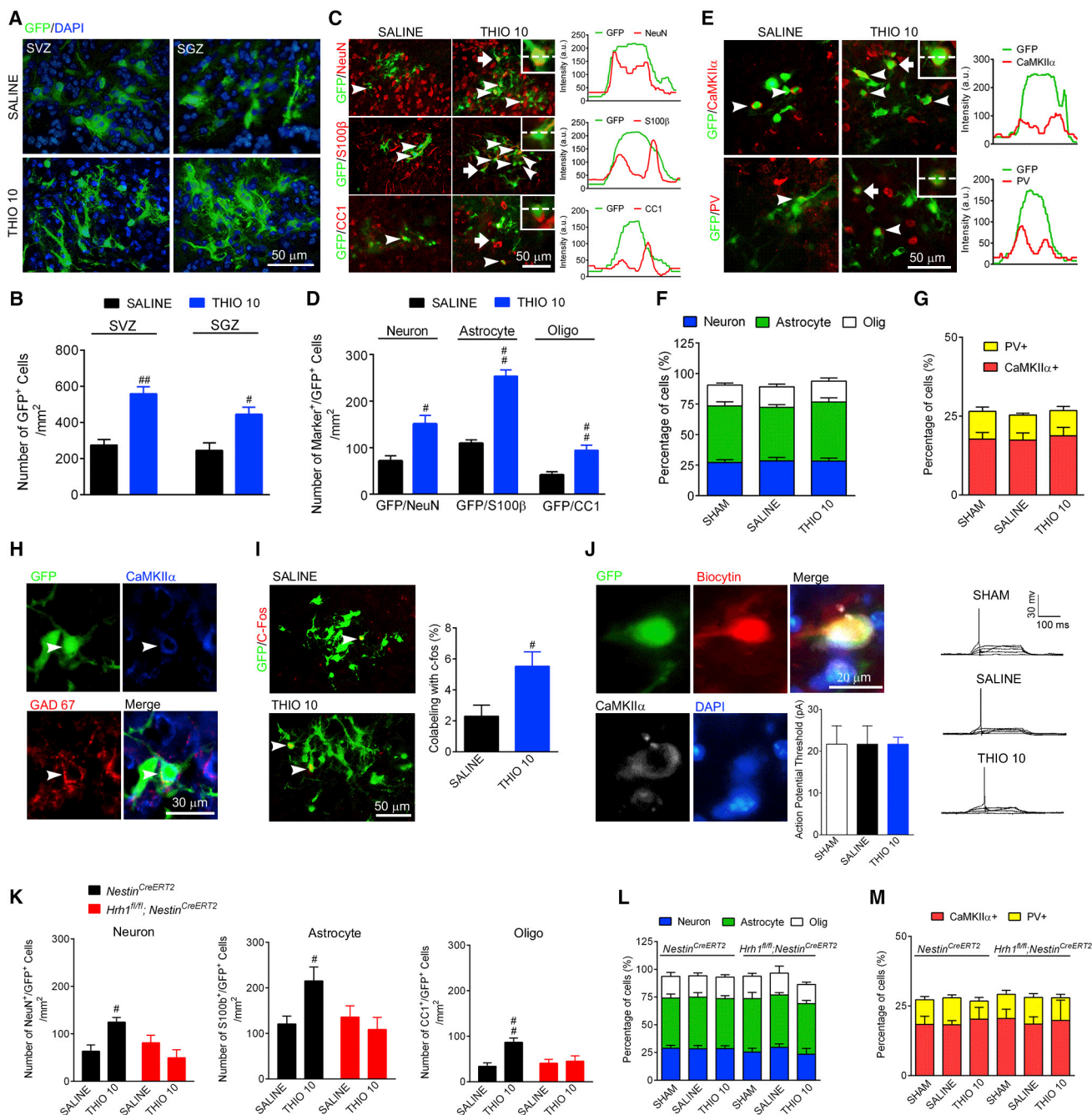
Figure 5. The H1R in Newly Generated Cells Is Critical for Differentiation into Functional Neural Cells Conferred by H3R Antagonism

The number of GFP$^+$ newly generated cells labeled with pROV-EF1a-GFP retrovirus injected into SVZ and SGZ were counted at the penumbral area at 28 days after cryogenic brain lesion in WT mice treated with thioperamide (THIO, 10 mg/kg/day, i.p.) or saline is shown in (B), with representative photographs in (A). The fate of these newly generated cells at the penumbral area was determined by counting the number of GFP$^+$ newly generated cells co-localized with NeuN, S100β, and CC1 (indicating neuron, astrocyte, and oligodendrocyte [Oligo], respectively), shown in (D), with representative photographs in (C), and their percentages are shown in (F). The numbers of newly generated CaMKIIα$^+$ glutamatergic neurons and PV$^+$ inhibitory neurons and their percentages were analyzed in (G), with representative photographs in (E). The line scan analysis of the fluorescence intensities of NeuN, S100, CC1, CaMKIIα, and PV together with GFP is shown along with representative photographs. The peak of NeuN, S100, CC1, CaMKIIα, and PV corresponding to the peak of GFP suggests

neurons and PV^{+} neurons (Figures 5E and 5G), which were comparable to those of the sham group. Furthermore, we found that the somas of those CaMKIIα^{+} glutamatergic neurons were surrounded by GAD67^{+} inhibitory synapses (Figure 5H), suggesting functional connections may be established in these newly generated neurons. c-Fos is known to be expressed in neurons in response to various physiological stimuli (Kee et al., 2007; Ohira et al., 2010), so we examined c-Fos expression in GFP-labeled, newly generated cells after H3R antagonism in WT mice that had received training in a Morris water maze. The percentage of GFP^{+} neurons that expressed c-Fos in the thioperamide group was much higher than in the saline group (Figure 5I), which suggests that more functional neurons are generated following H3R antagonism. To further detect the electrophysiological properties of newly generated neurons, the action potential threshold was determined through an electrophysiology study. The action potential threshold of newly generated neurons, either with or without thioperamide treatment, is comparable to that in the sham group (Figure 5J). These results suggest that at least some of the newly generated neuroblasts are differentiated into functional neurons. Furthermore, the increase in the number of newly generated neural cells was preserved in Nestin[CreERT2] mice after H3R antagonism, but disappeared in Hrh1^{fl/fl};Nestin[CreERT2] mice (Figure 5K). However, either the percentage of each type of neural cell or the percentage of the two main types of neurons remained the same in Nestin[CreERT2] mice and Hrh1^{fl/fl};Nestin[CreERT2] mice, regardless of whether or not they are treated with thioperamide (Figures 5L and 5M). Therefore the H1R in newly generated cells does not alter the differentiation pattern, but preserves a close-to-natural cell composition.

DISCUSSION

With the exception of rehabilitation, there is currently no other effective and available therapy to improve neurological outcomes for patients in the late phase of TBI. Various preclinical and clinical trials have been undertaken for H3R antagonists in the treatment of neurodegenerative diseases and sleep disorders (Hu and Chen, 2017; Schwartz, 2011). In the present study, we found that H3R antagonism shows prominent neuroprotection against TBI during its late phase, with a remarkable reduction of neurological dysfunction and lesion size (Figure 1). Moreover, the enhanced neurogenesis after H3R antagonism contributes to this neuroprotection, since more neuroblasts are generated and differentiate into mature and functional neurons in the area of the penumbra (Figures 2A, 2B, and 5A–5J) (Piao et al., 2013). Our study thus indicated that the H3R may serve as a promising target for the clinical treatment of TBI through a robust elevation of neurogenesis. Given the limited endogenous neurogenesis after TBI (Figures 2A and 2B), H3R antagonists may be good potential candidate drugs for neurological recovery.

Since both histamine-dependent and histamine-independent modes of action have been found to be related to the neuroprotection through H3R antagonism (Hu and Chen, 2012, 2017; Yan et al., 2014), we are interested in whether H3R antagonists promote neurogenesis in the context of TBI through activation of the histaminergic system. Our study demonstrates that the promotion of neurogenesis conferred by H3R antagonists is the result of activation of histaminergic neurons, since this improved neurological regeneration was completely halted when histamine was depleted by pharmacological treatments or by genetic blockage of histamine synthesis (Figures 2A and 2C). Although previous studies have implicated both the H1R and the H2R in the mechanism of action of histamine in neurogenesis (Molina-Hernandez and Velasco, 2008), the role of cell-type-specific postsynaptic histamine receptors in the present study is still unknown. We found that the H1R, but not the H2R, participates in the H3R antagonism-conferred neurogenesis and neuroprotection (Figures 2C–2F). To further investigate whether the NSC-specific H1R is involved in the action of neurological recovery, we generated Hrh1^{fl/fl};Nestin[CreERT2] and Hrh2^{fl/fl};Nestin[CreERT2] mice who have inducible and selective deletions of H1R or H2R in NSCs that otherwise do not affect embryonic and early postnatal development (Figure 3). Our results show that in NSCs, only the H1R, and not the H2R, is responsible for the promotion of neurogenesis and neuroprotection after TBI provided by H3R antagonism. In contrast, the glutamatergic excitatory projections are suggested to modulate neurogenesis during development and adulthood (Maithe Arruda-Carvalho et al., 2014;

co-localization. Images in (H) show GAD67^{+} synapse formation on the soma of CaMKIIα^{+} glutamatergic neurons in WT mice treated with THIO (10 mg/kg/day, i.p.) after TBI. Meanwhile, the numbers of GFP[+] newly generated cells co-labeled with c-Fos were counted at the penumbral area in mice after receiving Morris water maze training before sacrifice and are shown in (I). The electrophysiological properties of GFP[+] newly generated CaMKIIα^{+} neurons at the penumbral area are shown in (J). The fate of newly generated cells at the penumbral area in Hrh1^{fl/fl};Nestin[CreERT2] and their Nestin[CreERT2] littermates is shown in (K). The percentages of newly generated neural cells and the percentages of CaMKIIα^{+} glutamatergic neurons and PV^{+} inhibitory neurons in Hrh1^{fl/fl};Nestin[CreERT2] and their Nestin[CreERT2] littermates are shown in (L) and (M). (B, D, F, G–J) n = 6; (K–M) n = 4–6. [#]p < 0.05, [##]p < 0.01 versus the SALINE group. Arrowheads indicate the marker[+]/GFP^{+} cells. See also Figure S5.

Zhao et al., 2008). However, we found, using $Hrh1^{fl/fl}$; $CaMKII\alpha^{Cre}$ mice, that the H1R in CaMKIIα⁺ glutamatergic neurons is not involved in H3R antagonism-mediated neurogenesis (Figures S2B–S2D). This finding indicates that the regeneration of NSCs is largely mediated by a direct activation of endogenous H1R, rather than an indirect regulation of H1R in surrounding cells following H3R blockade. Taken together, our results suggest that, following TBI, H3R antagonism activates the histaminergic system and then H1R, but not H2R, in NSCs to boost neurogenesis and subsequent functional recovery.

Although histamine can induce both proliferation and differentiation *in vitro* (Molina-Hernandez and Velasco, 2008), the promotion of neurogenesis conferred by H3R antagonism here does not seem to be caused by either the proliferation or the reduction of apoptosis of NSCs (Figure S3). Furthermore, H3R antagonism enhances differentiation of neuroblasts with an elaborated morphology, having longer leading processes and longer total branches (Figures 4A and 4B). An effective neurogenesis relies not only on the eventual differentiation into mature neural cells, but also on the right composition of differentiated cells and functional integration (Li and Chen, 2016). Here, we found that those newly generated neuroblasts can differentiate into mature neural cells, including neurons, astrocytes, and oligodendrocytes (Figure 5C). Importantly, H3R antagonism elevated the number of each type of cell, without affecting their composition, which was comparable to that of the sham group (Figures 5C, 5D, and 5F). Such a normal cell composition may be critical for neurological repair, since excessive generation of one cell type may result in tumorigenesis (Buffo et al., 2008; Niu et al., 2013). Moreover, the simultaneous generation of excitatory and inhibitory neurons in the right composition could potentially balance excitation and inhibition (Guo et al., 2014). We further found that the composition of newly generated CaMKIIα⁺ glutamatergic neurons and PV⁺ inhibitory neurons, after H3R antagonist treatment, resembles that in the sham group (Figures 5E and 5G), suggesting that the H3R antagonism induces differentiation of the right neurons to achieve effective neurogenesis. In addition, the integrated interactions between functional neurons are fundamental for the recovery of neurological functions (Hagg, 2005). Indeed, we observed synaptic connections with surrounding neurons, functional responses, and the capacity to fire action potentials in newly generated neurons, which implies that functional integration can be established in those cells. H3 antagonism thus boosts neurogenesis by promotion of NSC differentiation into mature and functional neurons to provide neurological recovery following TBI.

In addition, this promotion of differentiation is manipulated by the H1R in NSCs, since the increased differentia-

tion is abrogated in $Hrh1^{fl/fl}$;$Nestin^{CreERT2}$ mice (Figures 4C, 4D, and 5K). It has been suggested that transcription of pro-neurogenic genes such as Mash1, Dlx2, and Neurogenin1 is related to the neurogenic effect of H1R *in vitro* (Bernardino et al., 2012; Rodriguez-Martinez et al., 2012). However, the determination of whether these proteins are involved in the action of H1R in this process requires further study since different NSC differentiation patterns have been observed between the present study and previous *in vitro* research. For example, in cultured NSCs, histamine reportedly favors neuron commitment during differentiation through H1R (Molina-Hernandez and Velasco, 2008), although we found the H1R in NSCs does not skew the differentiation pattern, but preserves a close-to-natural cell composition that could be critical for neurological recovery.

In conclusion, the present study showed that H3R antagonism confers a neuroprotection against TBI, in the late phase, through a promotion of neurogenesis; activation of the histaminergic system and subsequently the H1R in NSCs is required for this protection. Our findings shed light on the promising therapeutic role of H3R for TBI. With the current lack of convenient approaches for neurogenesis, H3R antagonism can be a simple and effective solution to promote significant neurogenesis during neurological recovery following TBI.

EXPERIMENTAL PROCEDURES

Animals

Male mice from the C57BL/6 strain, 8 to 12 weeks old, including WT, $HDC^{-/-}$, $Hrh3^{-/-}$, $Nestin^{CreERT2}$, $Hrh1^{fl/fl}$;$Nestin^{CreERT2}$, and $Hrh2^{fl/fl}$;$Nestin^{CreERT2}$ genotypes, were used. The $Hrh3^{-/-}$ mice were supplied by Johnson & Johnson Pharmaceutical Research & Development (La Jolla, CA) and were bred and maintained by The Jackson Laboratory. The $HDC^{-/-}$ mice were kindly provided by Professor Hiroshi Ohtsu, Department of Engineering, School of Medicine, Tohoku University (Liu et al., 2007), and $Nestin^{CreERT2}$ were kindly provided by Professor Mengsheng Qiu, College of Life Sciences, Hangzhou Normal University. $Hrh1^{fl/fl}$;$Nestin^{CreERT2}$ and $Hrh2^{fl/fl}$;$Nestin^{CreERT}$ mice were obtained by breeding $Hrh1^{fl/fl}$ mice or $Hrh2^{fl/fl}$ mice with $Nestin^{CreERT2}$ mice. $Hrh1^{fl/fl}$ mice or $Hrh2^{fl/fl}$ mice were generated by standard homologous recombination commercially at the Nan Jing Biomedical Research Institute of Nanjing University (Nanjing, China). Exon 3, encoding the core region of $Hrh1$, and exon 2, encoding the core region of $Hrh2$, were both flanked on either side by *loxP* sequences. $Hrh1^{fl/fl}$; $Nestin^{CreERT2}$ and $Hrh2^{fl/fl}$;$Nestin^{CreERT}$ mice were injected intraperitoneally with 2 mg of tamoxifen (Sigma-Aldrich, USA) once per day for 5 consecutive days before the surgery, as previously described (Giachino et al., 2014; Sahay et al., 2011), to induce the selective deletion of $Hrh1$ or $Hrh2$ in Nestin-expressing NSCs. All experiments and protocols were approved by the Zhejiang University Animal Experimentation Committee and were in complete

compliance with the National Institutes of Health *Guide for the Care and Use of Laboratory Animals*. Throughout the TBI performance, behavioral testing, and histological analysis, experimenters were blinded to the experimental conditions of the animals.

Cryogenic Brain Lesion Model

As previously described (Campbell et al., 2012; Chen et al., 2014), mice were subjected to a cryogenic brain lesion after anesthesia by intraperitoneal injection of sodium pentobarbital (50 mg/kg). A cryogenic brain lesion was inflicted using a 3-mm-diameter metal rod supercooled with liquid nitrogen. The metal rod was placed on the skull with the center of the rod at 1 mm behind the bregma and 1.5 mm right lateral. The rod was left in place for 15 s causing focal injury. Uninjured control mice were surgically prepared in a similar manner, but not subjected to injury. After the surgery, the scalp was sutured and the mice were allowed to recover in a recovery chamber at 37°C.

Controlled Cortical Impact Model

The CCI model was performed as previously reported (Glushakov et al., 2014; Sabirzhanov et al., 2016). An incision was made in the scalp, and the skull was exposed. CCI was stereotaxically induced using a PCI3000 PinPoint Precision Cortical Impactor (Hatteras Instruments, Cary, NC, USA) with the following parameters: 3-mm-diameter impact tip, 3 m/s velocity, 120 ms contusion time, and 2 mm contusion depth, allowing us to create a reproducible, experimental contusive TBI model with mild-to-moderate severity. Sham mice underwent the same anesthesia and craniotomy surgery procedures, but not CCI. Following injury, the mice were housed in a recovery chamber at 37°C.

Assessment of Functional Outcome

Neurological function was evaluated 1 day before the surgery and at 1, 7, 14, 21, and 28 days after surgery using a beam walk test and a wire hanging test (Fujimoto et al., 2004; Kabadi et al., 2010). Beams are horizontal and 50 cm above the table. A bright light illuminates the start area. An enclosed escape box, 20 cm³, is at the end of the beam. The time to traverse the 1-cm-wide beam is averaged from three trials on the indicated test days. For the wire hanging test, we used a standard wire cage lid that measured the balance and grip strength of the animal while gripping the wire cage lid. Briefly, the mouse is placed on the top of a wire cage lid. The investigator shakes the lid lightly to cause the mouse to grip the wires, and then turns the lid upside down. The upside-down lid is high enough to prevent the mouse from easily climbing down but not to cause harm in the event of a fall. The investigator uses a stopwatch to quantitate the latency to fall off the wire lid. A 60-s cutoff time is used for both behavioral tests.

Drug Administration

Animals were intraperitoneally injected with the H3R antagonist thioperamide (2, 5, or 10 mg/kg/day, Sigma-Aldrich, USA) within 1 h of and then once per day after TBI. The H1R antagonist pyrilamine (10 mg/kg/day, Sigma-Aldrich, USA) and H2R antagonist cimetidine (10 mg/kg/day, Sigma-Aldrich, USA) were intraperitoneally injected 15 min before treatment with thioperamide.

α-FMH (5 μg/day in saline, intracerebroventricularly [i.c.v.]) (Provensi et al., 2014) or the H3R agonist immepip (1 μg/day in saline, Sigma-Aldrich, USA, i.c.v.) was given at 15 min before treatment with thioperamide.

Assessment of Lesion Volume

To quantify the lesion volume, serial coronal brain sections were cut at 30 μm on a cryostat (Leica, Germany) and collected every 300 μm. The slices were stained with Giemsa stain (Sigma-Aldrich, USA) as described previously (Liao et al., 2015). The lesion volume, defined as the volume showing reduced Giemsa staining under light microscopy, was traced and quantified by ImageJ (Chen et al., 2014).

Immunohistochemistry Staining

Mice were transcardially perfused with a solution containing 0.9% NaCl at 4°C, followed by 4% paraformaldehyde in 0.1 M phosphate buffer (pH 7.4). Brains were removed and postfixed by incubation in 4% paraformaldehyde at 4°C overnight. Brains were cryoprotected by incubation in 30% sucrose in saline for 48 h. Coronal sections of brain tissue, 20 μm thick, were obtained using a cryostat (CM 3050S, Leica) and were thaw-mounted onto coated glass slides. Nonspecific staining was blocked by 5% donkey serum. Slices were first incubated with primary antibodies at 4°C overnight and then with Alexa Fluor-conjugated secondary antibodies (no. 711-545-152, 715-585-150, 715-585-152, or 715-605-151; Jackson ImmunoResearch Laboratories) at room temperature. DAPI, 1:1,000 (Sigma-Aldrich, USA), was used as a nuclear stain. Primary antibodies used in this study were as follows: rabbit anti-DCX (1:500, CST, USA, no. 4604s), mouse anti-PSA-NCAM (1:200, Millipore, USA, no. MAB5324), rabbit anti-NeuN (1:1,000, Millipore, USA, no. MABN140), mouse anti-s100β (1:200, Boster, China, no. BM0120), mouse anti-CC1 (1:400, Abcam, USA, no. ab16794), mouse anti-CaMKIIα (1:400, Abcam, USA, no. ab22609), mouse anti-c-Fos (1:400, Abcam, USA, no. ab208942), mouse anti-GAD67 (1:400, Millipore, USA, no. MAB5406), and rabbit anti-PV (1:500, Swant, Switzerland, no. PV27). All sections were observed under a confocal microscope (FV1000, Olympus, Japan). Merge-channel views were acquired with the associated FV10-ASW 2.1 Viewer software. All quantifications of labeled cells were carried out at a similar coronal position. Line-scan analysis of the fluorescence intensity was performed to confirm the co-localization.

Retrovirus Injection

A pROV-EF1a-GFP retrovirus (Hesp et al., 2015) (Neuron Biotech, China) was used to trace newborn cells, by direct injection of the virus in the ipsilateral SVZ (AP −1.5 mm, RL 2.0 mm, H −2.2 mm) or SGZ (AP −1.5 mm, RL 1.0 mm, H −2.2 mm). A volume of 1 μL of GFP-retrovirus solution (titer 4 × 10⁸ colony-forming units/mL) was carefully drawn up into a sterile Hamilton syringe at day 5 before TBI. Mice were sacrificed 28 days after TBI, and coronal tissue sections were obtained for immunostaining with NeuN, CC-1, S100β, c-Fos, PV, CaMKII, or GAD67 as mentioned above. For c-Fos immunostaining, mice were subjected to a Morris water maze test before sacrifice, as previously described (Ohira et al., 2010).

Electrophysiology

The brain was quickly removed and immersed in ice-cold artificial cerebrospinal fluid (containing 130 mM NaCl, 1.25 mM KCl, 0.25 mM CaCl$_2$, 3.5 mM MgCl$_2$, 0.65 mM NaH$_2$PO$_4$, 12.5 mM NaHCO$_3$, 55 mM choline chloride, 10 mM glucose, 0.65 mM ascorbic acid, and 0.3 mM sodium pyruvate), which was constantly bubbled with 95% O$_2$ and 5% CO$_2$. Coronal striatal slices at 300-μm thickness were cut using a Vibratome (VT1000 mol/L/E, Leica) and incubated at 25°C for 1 h. The slices were transferred into a recording chamber at 25°C for patch-clamp recording. The patch pipette (5-10 mol/LΩ resistance) was filled with recording solution (containing 120 mM potassium gluconate, 10 mM KCl, 1 mM NaCl, 1 mM MgCl$_2$, 1 mM CaCl$_2$, 10 mM EGTA, 2 mM Mg-ATP, 0.3 mM Na-GTP, 10 mM HEPES, and 2 mM biocytin). Signals were amplified and recorded by an HEKA EPC10 amplifier (HEKA Instruments, Germany). To test the action potential threshold of neurons being recorded, episodic currents, from 0 pA to depolarizing 100 pA at steps of 5 pA, were injected under the current-clamp configuration. Recorded neurons are filled with biocytin (Sigma-Aldrich, USA) and visualized with Alexa 555-streptavidin (Invitrogen, USA, no. S32355).

Statistical Analysis

Data are presented as the mean ± SEM. Multiple comparisons were analyzed by one-way ANOVA followed by Bonferroni's test, while two-tailed-Student's t test was applied for other comparisons between two groups. For all analyses, the tests were two-sided and p < 0.05 was considered statistically significant. "n" stands for the number of mice used in the experiment.

SUPPLEMENTAL INFORMATION

Supplemental Information includes Supplemental Experimental Procedures and five figures and can be found with this article online at https://doi.org/10.1016/j.stemcr.2019.01.004.

AUTHOR CONTRIBUTIONS

ACKNOWLEDGMENTS

REFERENCES

Bernardino, L., Eiriz, M.F., Santos, T., Xapelli, S., Grade, S., Rosa, A.I., Cortes, L., Ferreira, R., Braganca, J., Agasse, F., et al. (2012). Histamine stimulates neurogenesis in the rodent subventricular zone. Stem Cells 30, 773–784.

Blaya, M.O., Tsoulfas, P., Bramlett, H.M., and Dietrich, W.D. (2015). Neural progenitor cell transplantation promotes neuroprotection, enhances hippocampal neurogenesis, and improves cognitive outcomes after traumatic brain injury. Exp. Neurol. 264, 67–81.

Blennow, K., Hardy, J., and Zetterberg, H. (2012). The neuropathology and neurobiology of traumatic brain injury. Neuron 76, 886–899.

Buffo, A., Rite, I., Tripathi, P., Lepier, A., Colak, D., Horn, A.P., Mori, T., and Gotz, M. (2008). Origin and progeny of reactive gliosis: a source of multipotent cells in the injured brain. Proc. Natl. Acad. Sci. U S A 105, 3581–3586.

Campbell, M., Hanrahan, F., Gobbo, O.L., Kelly, M.E., Kiang, A.S., Humphries, M.M., Nguyen, A.T., Ozaki, E., Keaney, J., Blau, C.W., et al. (2012). Targeted suppression of claudin-5 decreases cerebral oedema and improves cognitive outcome following traumatic brain injury. Nat. Commun. 3, 849.

Chen, Z., Jalabi, W., Hu, W., Park, H.J., Gale, J.T., Kidd, G.J., Bernatowicz, R., Gossman, Z.C., Chen, J.T., Dutta, R., et al. (2014). Microglial displacement of inhibitory synapses provides neuroprotection in the adult brain. Nat. Commun. 5, 4486.

Escobedo-Avila, I., Vargas-Romero, F., Molina-Hernández, A., López-González, R., Cortés, D., De Carlos, J.A., and Velasco, I. (2014). Histamine impairs midbrain dopaminergic development in vivo by activating histamine type 1 receptors. Mol. Brain 7, 58.

Fujimoto, S.T., Longhi, L., Saatman, K.E., Conte, V., Stocchetti, N., and McIntosh, T.K. (2004). Motor and cognitive function evaluation following experimental traumatic brain injury. Neurosci. Biobehav. Rev. 28, 365–378.

Giachino, C., Barz, M., Tchorz, J.S., Tome, M., Gassmann, M., Bischofberger, J., Bettler, B., and Taylor, V. (2014). GABA suppresses neurogenesis in the adult hippocampus through GABAB receptors. Development 141, 83–90.

Glushakov, A.V., Fazal, J.A., Narumiya, S., and Dore, S. (2014). Role of the prostaglandin E2 EP1 receptor in traumatic brain injury. PLoS One 9, e113689.

Guo, Z., Zhang, L., Wu, Z., Chen, Y., Wang, F., and Chen, G. (2014). In vivo direct reprogramming of reactive glial cells into functional neurons after brain injury and in an Alzheimer's disease model. Cell Stem Cell 14, 188–202.

Haas, H., and Panula, P. (2003). The role of histamine and the tuberomamillary nucleus in the nervous system. Nat. Rev. Neurosci. 4, 121–130.

Hagg, T. (2005). Molecular regulation of adult CNS neurogenesis: an integrated view. Trends Neurosci. 28, 589–595.

Hallbergson, A.F., Gnatenco, C., and Peterson, D.A. (2003). Neurogenesis and brain injury: managing a renewable resource for repair. J. Clin. Invest. 112, 1128–1133.

Hesp, Z.C., Goldstein, E.Z., Miranda, C.J., Kaspar, B.K., and McTigue, D.M. (2015). Chronic oligodendrogenesis and remyelination after spinal cord injury in mice and rats. J. Neurosci. *35*, 1274–1290.

Hu, W., and Chen, Z. (2017). The roles of histamine and its receptor ligands in central nervous system disorders: an update. Pharmacol. Ther. *175*, 116–132.

Hu, W.W., and Chen, Z. (2012). Role of histamine and its receptors in cerebral ischemia. ACS Chem. Neurosci. *3*, 238–247.

Huang, Y.W., Hu, W.W., Chen, Z., Zhang, L.S., Shen, H.Q., Timmerman, H., Leurs, R., and Yanai, K. (2004). Effect of the histamine H3-antagonist clobenpropit on spatial memory deficits induced by MK-801 as evaluated by radial maze in Sprague-Dawley rats. Behav. Brain Res. *151*, 287–293.

Kabadi, S.V., Hilton, G.D., Stoica, B.A., Zapple, D.N., and Faden, A.I. (2010). Fluid-percussion-induced traumatic brain injury model in rats. Nat. Protoc. *5*, 1552–1563.

Kee, N., Teixeira, C.M., Wang, A.H., and Frankland, P.W. (2007). Preferential incorporation of adult-generated granule cells into spatial memory networks in the dentate gyrus. Nat. Neurosci. *10*, 355–362.

Levin, H.S., and Diaz-Arrastia, R.R. (2015). Diagnosis, prognosis, and clinical management of mild traumatic brain injury. Lancet Neurol. *14*, 506–517.

Li, H., and Chen, G. (2016). In vivo reprogramming for CNS repair: regenerating neurons from endogenous glial cells. Neuron *91*, 728–738.

Liao, R.J., Jiang, L., Wang, R.R., Zhao, H.W., Chen, Y., Li, Y., Wang, L., Jie, L.Y., Zhou, Y.D., Zhang, X.N., et al. (2015). Histidine provides long-term neuroprotection after cerebral ischemia through promoting astrocyte migration. Sci. Rep. *5*, 15356.

Liu, L., Zhang, S., Zhu, Y., Fu, Q., Zhu, Y., Gong, Y., Ohtsu, H., Luo, J., Wei, E., and Chen, Z. (2007). Improved learning and memory of contextual fear conditioning and hippocampal CA1 long-term potentiation in histidine decarboxylase knock-out mice. Hippocampus *17*, 634–641.

Maithe Arruda-Carvalho, L., Restivo, L., Guskjolen, A., Epp, J.R., Elgersma, Y., Josselyn, S.A., and Frankland, P.W. (2014). Conditional deletion of α-CaMKII impairs integration of adult-generated granule cells into dentate gyrus circuits. J. Neurosci. *34*, 11919–11928.

Molina-Hernandez, A., and Velasco, I. (2008). Histamine induces neural stem cell proliferation and neuronal differentiation by activation of distinct histamine receptors. J. Neurochem. *106*, 706–717.

Niu, W., Zang, T., Zou, Y., Fang, S., Smith, D.K., Bachoo, R., and Zhang, C.L. (2013). In vivo reprogramming of astrocytes to neuroblasts in the adult brain. Nat. Cell Biol. *15*, 1164–1175.

Ohira, K., Furuta, T., Hioki, H., Nakamura, K.C., Kuramoto, E., Tanaka, Y., Funatsu, N., Shimizu, K., Oishi, T., Hayashi, M., et al. (2010). Ischemia-induced neurogenesis of neocortical layer 1 progenitor cells. Nat. Neurosci. *13*, 173–179.

Piao, C.S., Stoica, B.A., Wu, J., Sabirzhanov, B., Zhao, Z., Cabatbat, R., Loane, D.J., and Faden, A.I. (2013). Late exercise reduces neuroinflammation and cognitive dysfunction after traumatic brain injury. Neurobiol. Dis. *54*, 252–263.

Provensi, G., Coccurello, R., Umehara, H., Munari, L., Giacovazzo, G., Galeotti, N., Nosi, D., Gaetani, S., Romano, A., Moles, A., et al. (2014). Satiety factor oleoylethanolamide recruits the brain histaminergic system to inhibit food intake. Proc. Natl. Acad. Sci. U S A *111*, 11527–11532.

Rodriguez-Martinez, G., Velasco, I., Garcia-Lopez, G., Solis, K.H., Flores-Herrera, H., Diaz, N.F., and Molina-Hernandez, A. (2012). Histamine is required during neural stem cell proliferation to increase neuron differentiation. Neuroscience *216*, 10–17.

Sabirzhanov, B., Stoica, B.A., Zhao, Z., Loane, D.J., Wu, J., Dorsey, S.G., and Faden, A.I. (2016). miR-711 upregulation induces neuronal cell death after traumatic brain injury. Cell Death Differ. *23*, 654–668.

Sahay, A., Scobie, K.N., Hill, A.S., O'Carroll, C.M., Kheirbek, M.A., Burghardt, N.S., Fenton, A.A., Dranovsky, A., and Hen, R. (2011). Increasing adult hippocampal neurogenesis is sufficient to improve pattern separation. Nature *472*, 466–470.

Schwartz, J.C. (2011). The histamine H3 receptor: from discovery to clinical trials with pitolisant. Br. J. Pharmacol. *163*, 713–721.

Smith, D.H., Soares, H.D., Pierce, J.S., Perlman, K.G., Saatman, K.E., Meaney, D.F., Dixon, C.E., and McIntosh, T.K. (1995). A model of parasagittal controlled cortical impact in the mouse: cognitive and histopathologic effects. J. Neurotrauma *12*, 169–178.

Trounson, A., and McDonald, C. (2015). Stem cell therapies in clinical trials: progress and challenges. Cell Stem Cell *17*, 11–22.

Xiong, Y., Mahmood, A., and Chopp, M. (2010). Angiogenesis, neurogenesis and brain recovery of function following injury. Curr. Opin. Investig. Drugs *11*, 298–308.

Xiong, Y., Mahmood, A., and Chopp, M. (2013). Animal models of traumatic brain injury. Nat. Rev. Neurosci. *14*, 128–142.

Yan, H., Zhang, X., Hu, W., Ma, J., Hou, W., Zhang, X., Wang, X., Gao, J., Shen, Y., Lv, J., et al. (2014). Histamine H3 receptors aggravate cerebral ischaemic injury by histamine-independent mechanisms. Nat. Commun. *5*, 3334.

Zhang, L., Chen, Z., Ren, K., Leurs, R., Chen, J., Zhang, W., Ye, B., Wei, E., and Timmerman, H. (2003). Effects of clobenpropit on pentylenetetrazole-kindled seizures in rats. Eur. J. Pharmacol. *482*, 169–175.

Zhao, C., Deng, W., and Gage, F.H. (2008). Mechanisms and functional implications of adult neurogenesis. Cell *132*, 645–660.